

Supplemental Material

Methods Each second-long experimental cycle has a 12 ms detection period, which consists of 20 μ s measurement times, a time window arbitrarily chosen to be much longer than the EIT lifetime to allow the continuous measurement of signal photons, interleaved with 20 μ s preparation times that ensure the atoms are optically pumped to the $|g\rangle$ state. For cross correlation measurements such as Fig.2(a) an average of approximately 8000 experimental cycles were used.

The temperature of the cloud in the dipole trap is about 120 μ K corresponding to a measured atomic decoherence rate of $\gamma_0/2\pi \simeq 100$ kHz, dominated by the Doppler broadening. The signal path detection efficiency is $q_s \simeq 0.3$ including the fiber coupling efficiency and photodetector quantum efficiency. The optical cavity has a waist size of 35 μ m, length of 13.7 mm, and out-coupling efficiency of 66%.

The single-photon Rabi frequency for σ^+ polarized light is $2g = 2\pi \times 2.5$ MHz. Thus, the single-atom cooperativity for an atom on the cavity axis (along z) at an antinode of the cavity standing wave is given by $\eta = 4g^2/\kappa\Gamma = 8.6 > 1$, i.e. the system operates in the strong coupling regime of cavity quantum electrodynamics. The cavity resonance frequency matches the atomic frequency $|d\rangle \rightarrow |e\rangle$

Detection and transmission probabilities. The probability to observe a probe photon when a cavity photon is present and a signal photon is propagating through the EIT window at $\tau = 0$ is given by [S20]

$$\varepsilon_0 = \frac{1}{4} \frac{\eta^2}{(1+\eta)^2} [1 - \exp(-\mathcal{D}/2\zeta)]^2, \quad (1)$$

where

$$\zeta = \left(1 + \frac{\gamma\Gamma}{\Omega^2}\right) \left(1 + \frac{\Omega^2/\kappa\Gamma + \gamma/\kappa}{1+\eta}\right). \quad (2)$$

Here, $\eta = 4.3$ is the spatially-averaged cavity cooperativity, \mathcal{D} is the effective optical density that overlaps with the cavity mode, Ω is the control Rabi frequency, $\kappa = 2\pi \times 140$ kHz is the decay rate of the cavity, $\gamma \simeq \gamma_c + \gamma_0$, $\gamma_0 \approx 2\pi \times 100$ kHz is atomic decoherence rate in the absence of cavity photons, γ_c is cavity-induced decoherence, and Γ is the Cs excited-state decay rate. The decoherence rate, γ_c , caused by cavity light scattering manifests itself as: (1) loss of atomic coherence given by $\langle n_c^{in} \rangle \kappa \eta / (1+\eta)^2$ where $\langle n_c^{in} \rangle$ is the mean σ^+ -polarized input cavity photon number, (2) reduction of signal transmission as a result of inhomogenous coupling of cavity light to atoms (see below). For the anti-correlation data shown in the inset of Fig. 2a, when we take into account the cavity blocking due to an atom in state $|d\rangle$, we obtain $4\varepsilon_0 = 0.1$ and a blocking probability for σ^+ light of $P = 1 - (1 - \sqrt{4\varepsilon_0})^2 = 0.55$. This is in good agreement

with the measured probability of $1 - g_{s\sigma^+}^{(2)}(0) = 0.59(7)$. A detailed theoretical treatment of the cavity interaction with atomic ensemble is given in Ref. [25].

In the nondestructive detection where horizontally-polarized cavity light is used, the detection probability is defined as the field amplitude of the transmitted σ^+ light, which interacts with atoms in state $|d\rangle$ as described in Ref. [23], combined with the field amplitude of σ^- light on the output polarization beamsplitter. The field amplitude addition results in the factor 1/4 in Eq. 1. In principle, this reduction can be avoided by impinging only σ^+ light onto an impedance-matched cavity and measuring the reflected photons. In our present lossy cavity, the reflection in the absence of signal photons causes a large background for the probe light.

Cavity-induced decoherence reduces the transmission probability of the signal photon and the EIT coherence time [S20]. The signal transmission in the presence of cavity photons is given by:

$$T_s = T_0 \exp\left(-\frac{\mathcal{D}}{1 + \Omega^2/\Gamma\gamma}\right) \quad (3)$$

where $T_0 = \exp\left(-\frac{\mathcal{D}'}{1 + \Omega'^2/\Gamma\gamma_0}\right)$ is the EIT transmission corresponding to atoms outside the cavity waist and \mathcal{D}' is the corresponding optical density.

An additional limit to the signal transmission is caused by the standing-wave nature of the cavity light in combination with the uniform distribution of atoms between nodes and antinodes of the cavity. Once the signal is detected, the spatial mode of the polation is projected onto the cavity mode resembling a grating imprinted onto the polariton structure. This effect leads to reduction in transmission of the signal. The overlap between the polariton before and after detection of a probe photon can be calculated as

$$\mathcal{F}_p = \frac{1}{\pi} \int_0^\pi \frac{\eta \cos^2(\theta)}{1 + \eta \cos^2(\theta)} d\theta = 1 - \frac{1}{\sqrt{1+\eta}} \quad (4)$$

where $\theta = kz$, k is the wave-number of cavity light and z is the position along the cavity axis. At large cooperativity, $\eta \gg 1$, the expected maximum transmission approaches 100%. For our system parameters this evaluates to about 70%.

Also, the atomic cloud extended beyond the cavity region introduces additional signal transmission loss. This is because the signal photon wave-packet is localized inside the cavity region upon detection of a probe photon and therefore its spectral bandwidth exceeds the EIT bandwidth. Hence, after detection via the cavity, the signal photon propagating through the EIT window experiences dispersion and loss. Our numerical simulations predicts a loss of 30% in signal transmission given the experimental parameters. In principle, this loss can be eliminated by removing atoms outside the cavity region.

Quantum correlation between probe and signal photons. The mean photon rate entering the cavity can

be calculated from the total detected photon rate exiting the cavity, $R_c^{s=0}$, in absence of signal photons as

$$\langle R_c^{in} \rangle = \frac{R_c^{s=0}}{q_d \left(\frac{\mathcal{T}}{\mathcal{T} + \mathcal{L}} \right)} \quad (5)$$

where $q_d = 0.3$ accounts for detection losses including fiber coupling, filter losses and photodetector quantum efficiency and $\frac{\mathcal{T}}{\mathcal{T} + \mathcal{L}} = 0.66$ is the cavity out-coupling efficiency with \mathcal{L} and \mathcal{T} being mirror loss and transmissivity, respectively. In the following, we combine q_d and the cavity out-coupling efficiency into a single parameter q_p . The mean cavity photon number in absence of signal photons is then $\langle n_c^{in} \rangle = R_c^{in} \tau_c$ where $\tau_c = (\kappa/2)^{-1}$. The mean signal photon number in the relevant time window, i.e. the EIT life time $\tau_{EIT} = (\Omega^2/(\Gamma\mathcal{D}) + \gamma_0)^{-1}$, is given by $\langle n_s^{in} \rangle = R_s^{in} \tau_{EIT}/q_s$ where R_s^{in}/q_s is the signal photon rate entering the medium and $q_s = 0.3$ accounts for detection losses. In absence of population in state $|d\rangle$, the linearly polarized cavity light is rotated by atoms in state $|g\rangle$ due to the differences in the coupling strengths for σ^+ and σ^- polarized light interacting with state $|g\rangle$ and excited states. Ideally, this rotation is constant and we compensate for it with a waveplate at the output of the cavity. However, the shot-to-shot atom number fluctuation during loading provides a varying background, $\alpha q_p \langle n_c^{in} \rangle$, that dominates the probe port at low signal photon rates. We typically measure a maximum fractional background of $\alpha \approx 3 \times 10^{-3}$ of the total detected cavity photons. The detection events consists of a background given by $\langle b \rangle = \alpha q_p \langle n_c^{in} \rangle + \langle r_p \rangle$, where $\langle r_p \rangle$ denotes the dark counts of the probe detector D_p . We define the detected mean signal photon number $\langle n_s \rangle$, true detection events $\langle t \rangle$ and total detected mean probe photon number $\langle n_p \rangle$ as

$$\langle n_s \rangle = q_s T_s \langle n_s^{in} \rangle + \langle r_s \rangle \quad (6)$$

$$\langle t \rangle = (\varepsilon_0 + \epsilon_b) q_p \langle n_c^{in} \rangle \langle n_s^{in} \rangle \quad (7)$$

$$\langle n_p \rangle = \langle t \rangle + \langle b \rangle = (\varepsilon_0 \langle n_s^{in} \rangle + \epsilon_b \langle n_s^{in} \rangle + \alpha) q_p \langle n_c^{in} \rangle + \langle r_p \rangle \quad (8)$$

where $\langle r_s \rangle$ denotes the dark-counts of the signal detector D_s and $\epsilon_b = \varepsilon_d f_s$ is the probability of detecting a probe photon for a decohered atoms in state $|d\rangle$, ε_d , multiplied by the fraction of signal photons, f_s , incoherently mapped to state $|d\rangle$ via absorption. The coincidence counts are

$$\langle n_s n_p \rangle = \varepsilon_0 q_p \langle n_c^{in} \rangle \times T_s q_s \langle n_s^{in} \rangle + \quad (9)$$

$$\begin{aligned} & (\alpha + \epsilon_b \langle n_s^{in} \rangle) q_p \langle n_c^{in} \rangle \times T_s q_s \langle n_s^{in} \rangle + \\ & T_s q_s \langle n_s^{in} \rangle \langle r_p \rangle + ((\varepsilon_0 + \epsilon_b) \langle n_s^{in} \rangle + \\ & \alpha) \times q_p \langle n_c^{in} \rangle \langle r_s \rangle + \langle r_p \rangle \langle r_s \rangle. \end{aligned} \quad (10)$$

Here, we assume that the conditional signal transmission is approximately equal to the mean signal transmission, T_s . Note that all terms, except the first, are caused by

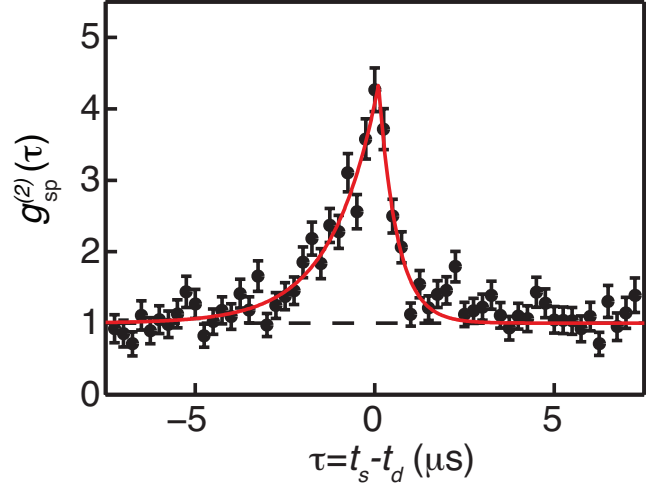


FIG. S1. Observed cross-correlation for double-pass signal beam, measured with $\langle n_c^{in} \rangle = 4.4$ and $\Omega/2\pi = 2.9$ MHz. The fitted values are $g^{(2)} = 4.4(5)$, $\tau_< = 1.3(3)$ μ s, and $\tau_> = 0.5(2)$ μ s.

background sources. The cross-correlation function, neglecting the detectors' dark counts, can be approximated as

$$g^{(2)}(\tau = 0) = \frac{\langle n_s n_p \rangle}{\langle n_s \rangle \langle n_p \rangle} \simeq \frac{1 + \beta}{\beta + \langle n_s^{in} \rangle} \quad (11)$$

where $\beta = \frac{\alpha + \epsilon_b \langle n_s^{in} \rangle}{\varepsilon_0}$. When background processes are negligible ($\alpha, \epsilon_b, \langle r_s \rangle, \langle r_p \rangle \ll 1$), the maximum cross-correlation function at $\tau = 0$ is simply approximated by $g^{(2)} \simeq 1/\langle n_s^{in} \rangle$ for $\langle n_s^{in} \rangle < 1$. Note that in the regime where $\langle r_s \rangle, \langle r_p \rangle \ll 1$, the correlation function $g^{(2)}$ is independent of the cavity photon number as both the detection probability and background scale linearly with it. However, the measured $g^{(2)}(\tau = 0)$ drops at low cavity photon numbers where probe-part dark counts, $\langle r_p \rangle$, are not negligible compared to the detected cavity mean photon number.

To further increase the photon-photon interaction, we carried out an experiment to increase the effective optical density by transmitting the signal through the atomic ensemble twice. The retro-reflected signal is collected by a 90/10 fiber-beam splitter used at the signal input. We simultaneously measure auto-correlations of $g_{ss}^{(2)} = 1.6(3)$, $g_{pp}^{(2)} = 5.6(1)$ and the cross-correlation as plotted in Fig. S1.

Quantum efficiency. The conditional nondestructive quantum efficiency of detecting a signal photon with mean input photon number $\langle n_s^{in} \rangle \ll 1$ can be written as

$$Q = \varepsilon q_p \langle n_c^{in} \rangle \simeq \frac{\langle n_s n_p \rangle - \langle n_p \rangle \langle n_s \rangle}{\langle n_s \rangle} \quad (12)$$

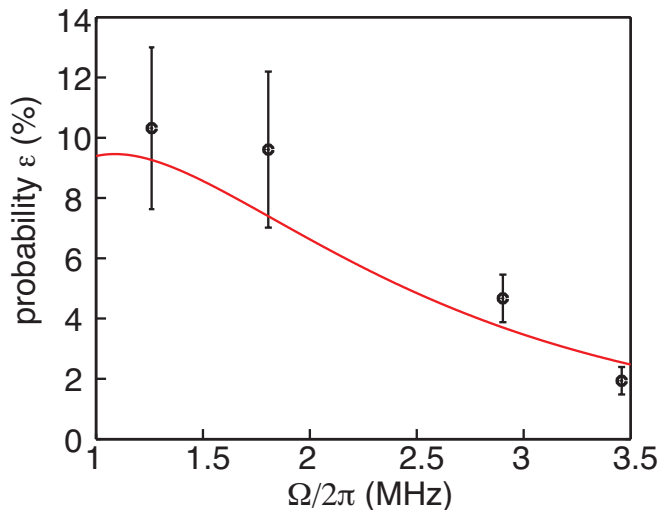


FIG. S2. The total probability ε calculated from the slope of the linear fits to the data in Fig. 3. The fitted curve represents the theory using Eq.13 with fitted optical density $\mathcal{D} = 4(2)$.

where ε is the total probability of having a probe photon given a signal photon traveling through the medium. It can be obtained from the asymptotic quantum efficiency and integrating the area under the $g^{(2)}$ function as

$$\begin{aligned} \varepsilon &= \frac{Q}{q_p \langle n_c^{in} \rangle} = \frac{1}{q_p \langle n_c^{in} \rangle (1 - \langle n_s^{in} \rangle)} \int (g^{(2)}(\tau) - 1) R_p d\tau \\ &= \varepsilon_0 \frac{\tau_c + \tau_{EIT}}{\tau_c}. \end{aligned} \quad (13)$$

The probability ε is calculated from the slope of the fitted lines in Fig. 4c and is plotted for different control Rabi frequencies in Fig. S2. These extracted probabili-

ties agree with theoretical predictions.

Detection probabilities and QND requirements.

The QND requirements can be quantified using the measurement error, ΔX , the transfer coefficient of input signal to meter (probe), \mathcal{T}_M , and transfer coefficient of input signal to output signal, \mathcal{T}_S [S13]. Using the formalism provided by Ralph *et al.* [Phys. Rev. A **73**, 012113 (2006)], one can link the measurement probabilities in the discrete variable (DV) regime and \mathcal{T}_S and \mathcal{T}_M in continuous variable (CV) regime through different fidelity measures. The transfer coefficients in terms of measurement fidelity, F_M , and QND fidelity, F_{QND} , can be written as

$$\begin{aligned} \mathcal{T}_M &= \left(\frac{2}{F_M^2} - 1 \right)^{-1} \\ \mathcal{T}_S &= \left(\frac{2}{F_{QND}^2} - 1 \right)^{-1} \end{aligned}$$

where

$$\begin{aligned} F_M &= P_{11} + P_{01} = \frac{\langle n_p \rangle}{\langle n_s^{in} \rangle} \\ F_{QND} &= P_{11} + P_{10} = T_s. \end{aligned}$$

To estimate the measurement error in the CV regime, the conditional variance of the signal is measured and is compared to the shot-noise limit. In the DV regime, however, as the particle aspect of photons are detected and not the wave aspect, the conditional correlation function, $g_{ss|m}^{(2)}$ (signal auto-correlation function conditioned on detecting a meter photon), can be used instead to quantify the measurement error. In particular, a QND measurement satisfies $g_{ss|m}^{(2)} < 1$ (quantum state preparation) and $\mathcal{T}_S + \mathcal{T}_M > 1$.